JBC Papers in Press. Published on June 19, 2002 as Manuscript M203494200

Rad52 protein associates with RPA-ssDNA to accelerate Rad51-mediated displacement of RPA and presynaptic complex formation.

Tomohiko Sugiyama and Stephen C. Kowalczykowski*

Sections of Microbiology and of Molecular and Cellular Biology,

and Center for Genetics and Development,

University of California, Davis,

Davis, California 95616-8665

***Corresponding Author:**

Section of Microbiology

Hutchison Hall

University of California, Davis

Davis, California 95616-8665

Phone: (530) 752-5938; Fax: (530) 752-5939

Electronic mail: sckowalczykowski@ucdavis.edu

Running title: Rad52-RPA-DNA complex facilitates Rad51 function

Summary

The Rad51 nucleoprotein filament mediates DNA strand exchange, a key step of homologous recombination. This activity is stimulated by RPA, but only when RPA is introduced after Rad51 nucleoprotein filament formation. In contrast, RPA inhibits Rad51 nucleoprotein complex formation by prior binding to ssDNA, but Rad52 protein alleviates this inhibition. Here we show that Rad51 filament formation is simultaneous with displacement of RPA from ssDNA. This displacement is initiated by a rate-limiting nucleation of Rad51 protein onto ssDNA complex, followed by rapid elongation of the filament. Rad52 protein accelerates RPA displacement by Rad51 protein. This acceleration likely involves direct interactions with both Rad51 protein and RPA. Detection of a Rad52-RPA-ssDNA co-complex suggests that this co-complex is an intermediate in the displacement process.

Introduction

The Rad52 epistasis group of proteins, including Rad51 protein, Rad52 protein, and replication protein-A (RPA), are important for both mitotic and meiotic recombination, mating-type switching, and repair of DNA double-strand breaks (DSBs) in *Saccharomyces cerevisiae*. Rad51 protein, which is a homologue of the *Escherichia coli* RecA protein (1-3), is conserved in a wide variety of eukaryotic organisms from yeast to human (4). Like RecA protein, Rad51 protein binds ssDNA to form the functional presynaptic complex which mediates DNA strand exchange (5). However, unlike RecA protein, Rad51 protein readily binds dsDNA, and the binding to dsDNA strongly inhibits DNA strand exchange (6). Therefore, not unexpectedly, the binding of Rad51 protein to dsDNA present as secondary structure in ssDNA severely limits DNA strand exchange (7). For this reason, Rad51 protein-mediated DNA strand exchange depends strongly on a ssDNA-binding protein to eliminate DNA secondary structure.

Replication protein-A (RPA), which is a heterotrimeric ssDNA-binding protein (8,9), greatly stimulates DNA strand exchange by Rad51 protein, provided that RPA is added to a pre-existing complex of Rad51 protein and ssDNA (5). However, RPA will inhibit DNA strand exchange when it is allowed to bind ssDNA before Rad51 protein. Previously, we offered an interpretation for this dichotomous role of RPA in Rad51 protein-mediated DNA strand exchange (7). According to this view, RPA aids DNA strand exchange by disrupting DNA secondary structure which is an impediment to presynaptic complex formation. However, because RPA and Rad51 protein both compete for these same ssDNA binding sites, RPA can also be an impediment to presynaptic complex formation. Nevertheless, when the molecular ratios of Rad51

protein and RPA to ssDNA are appropriate (2 - 3 nucleotide per Rad51 protein and 10 - 20 nucleotide per RPA), the steady-state product of this competitive process is a uniform Rad51 protein-ssDNA complex with little DNA secondary structure. Based on this model, after disruption of DNA secondary structure, RPA is expected to be displaced by Rad51 protein. Previously, however, we did not directly demonstrate the release of RPA from ssDNA.

Purified yeast Rad52 protein has DNA binding activity (10), and it also interacts with both Rad51 protein and RPA (1,11). Recent biochemical studies show that Rad52 protein has at least two activities important to recombination. One activity is the stimulation of Rad51 protein-mediated DNA strand exchange (12-15). Both Rad52 protein-RPA and Rad52 protein-Rad51 protein interactions are necessary for stimulation. This stimulatory function of Rad52 protein, however, is revealed under conditions where RPA inhibits Rad51 protein activity: *i.e.,* when RPA is bound to ssDNA prior to Rad51 protein. Therefore, it was hypothesized that Rad52 protein acts by stimulating the displacement of RPA by Rad51 protein (14). The second activity of Rad52 protein is the annealing of complementary ssDNA (10). This activity is consistent with the importance of this protein in the ssDNA annealing pathway of DSB repair (16). Yeast Rad52 protein can also anneal ssDNA that is complexed with yeast RPA, due to a specific interaction with RPA (11,17).

The precise mechanism by which Rad52 protein stimulates DNA strand exchange is not clear. Because Rad52 protein stimulates DNA strand exchange when RPA is pre-bound to ssDNA, Rad52 might simply displace RPA from the ssDNA, permitting Rad51 protein to bind. In this paper, we examine the fate of RPA during

presynaptic complex formation. Our results indicate that Rad52 protein alone cannot displace RPA from ssDNA. Instead, Rad52 protein forms a co-complex with the RPA-ssDNA complex, and it recruits the Rad51 protein onto ssDNA, and then Rad51 protein displaces RPA. Our results also reveal the dynamic nature of the complex protein exchange and assembly process, that underlies DNA recombination.

Experimental Procedures

DNA and Proteins

Poly(dT) was purchased from Pharmacia. The 100-mer synthetic DNA 5'-TGGCCTGCAA CGCGGGCATC CCGATGCCGC CGGAAGCGAG AAGAATCATA ATGGGGAAGG CCACCAGCCT CGCGTCGCGA ACGCCAGCAA GACGTAGCCC was purchased from Operon and purified by electrophoresis using 7.5% polyacrylamide gels containing 7 M urea. The 100-mer was labeled with ^{32}P at its 5'-end by T4-polynucleotide kinase (New England Biolabs). Bluescript SK- dsDNA and ssDNA (Stratagene) were prepared as described (18). The nucleotide concentrations of poly(dT), ssDNA, and dsDNA were measured using extinction coefficients of 7.3×10^3, 8.1×10^3 and 6.5×10^3 $M^{-1}cm^{-1}$, respectively. Rad51 and Rad52 proteins (14), RPA (19), *E. coli* SSB protein (20,21) were prepared as described. Rabbit polyclonal antibody against RPA was obtained from W. D. Heyer (Univ. California, Davis).

ATPase assay

ATP hydrolysis by Rad51 protein was analyzed at 37°C essentially as described (7,22). For the standard reaction, 10 μM of ssDNA, 5 μM Rad51 protein, and 1 μM of RPA were added in the indicated order to buffer (final volume of 120 μl) containing 2.5 mM ATP, 10 U/ml pyruvate kinase, 10 U/ml lactate dehydrogenase, 0.3 mM phosphoenolpyruvate, 256 μM NADH, 50 μg/ml bovine serum albumin, 1 mM dithiothreitol, 5 mM magnesium acetate, 50 mM KCl, and 30 mM Tris-acetate (pH 7.5). The hydrolysis of ATP is coupled to the oxidation of NADH, which results in a decrease in absorbance at 340 nm. The decrease of absorbance was monitored every 25

seconds by a Hewlett Packard 8452A diode array spectrophotometer. The instantaneous rate of ATP hydrolysis was calculated from the rate of change in absorbance based on 5 to 6 time-points using the formula: rate of A_{340} decrease (sec^{-1}) X 9880 = rate of ATP hydrolysis (μM/min). For Figure 2, we used 2.4 mM magnesium acetate instead of 5 mM, because the displacement was slower and the result was more apparent under these conditions (data not shown).

DNA binding by RPA monitored by fluorescence quenching

RPA has an intrinsic fluorescence that is quenched when it binds to ssDNA (19). On the other hand, Rad51 protein, which has no tryptophan residue, has much lower fluorescence (approximately 50-fold lower per molecule than RPA), and it does not change upon DNA binding (data not shown). Although Rad52 protein has approximately 40% of fluorescence of RPA, the fluorescence is unchanged by interaction with either ssDNA, Rad51, or RPA (data not shown). Therefore, the dissociation of RPA from ssDNA in the presence of Rad51 protein can be monitored in real time by monitoring the intrinsic fluorescence quenching of RPA. Reactions were done in a quartz cuvette containing 300 μl or 400 μl of buffer containing 2.5 mM ATP, 1 mM dithiothreitol, 5 mM magnesium acetate, 50 mM KCl, and 30 mM Tris-acetate (pH 7.5) at 37 °C. RPA (1 μM), ssDNA (10 μM), and Rad51 protein (5 μM) were added in the order indicated. Between each addition of protein or DNA, the components were allowed to equilibrate for 1.5 to 2 min. When indicated, Rad52 protein (1 μM) was added to the reaction mixture approximately 30 sec after addition of Rad51 protein. Throughout the reaction, the fluorescence of RPA was continuously monitored with an

SLM8000 spectrofluorimeter set to excitation and emission wavelengths of 284 nm and 345 nm, respectively. The band-width for excitation and emission was 1 and 4 nm, respectively. The percentage of RPA that was displaced from ssDNA was calculated from the fluorescence value relative to free RPA. The contributions of Rad51 and Rad52 proteins to the fluorescence were subtracted.

Gel mobility-shift assay

Proteins were mixed with 10 μM of ^{32}P-labeled synthetic 100-mer ssDNA in the indicated order, and incubated for 15 min at 37 °C in 10 μl of buffer containing 30 mM K-MOPS (pH 7.3), 20 mM NaCl, 3 mM magnesium acetate, 1 mM DTT, and 2 mM ATP (when indicated). When more than one protein was present, the samples were incubated for 10 min at 37 °C between each addition, and for 15 min after addition of the last protein. After the reaction, samples were analyzed by one of the following electrophoresis methods. For "conventional" electrophoresis, samples were mixed with 5 or 10 μl of loading buffer A (50% glycerol and 0.1% bromophenol blue in TBE buffer (45 mM Tris-borate (pH 8.3) and 1 mM EDTA)) and separated with 6% polyacrylamide gel in TBE buffer. Alternatively, electrophoresis was conducted in the presence of ATP and Mg^{++} : samples were mixed with 10 μl of the loading buffer B (50% glycerol, 20 mM NaCl, 5 mM magnesium acetate, 0.5 mM ATP, 0.1% bromophenol blue, and 45 mM Tris-borate (pH 8.3), and separated with 6% polyacrylamide gel in 20 mM KCl, 5 mM magnesium acetate, 0.5 mM ATP, and 45 mM Tris-borate (pH 8.3). For both methods, retardation of the labeled ssDNA was detected using Molecular Dynamics Storm 840 phospho-imager with Image-QuaNT software.

Quantification of protein-ssDNA complexes by SDS-PAGE.

The protein content of complexes detected in the gel-mobility shift experiments was analyzed in the following way. Gel-pieces containing protein-ssDNA complexes were excised, cut into smaller pieces, and then radioactivity was quantified by Cerenkov counting to measure the amount of ssDNA in each sample. Based on the relative radioactivity, number of pieces used for SDS-PAGE were adjusted so that all samples had the same radioactivity. That enabled comparison of the amount of protein present, normalized to the ssDNA content. The gel pieces (approximate volumes of 10 μl to 50 μl) were then mixed with 50 μl of TE buffer and 20 μl of SDS loading buffer (350 mM Tris-HCl (pH 6.8), 1% SDS, 6% 2-mercaptoethanol, 36% glycerol, and 0.1% bromophenol blue) and incubate for 3 hours at room temperature and then 4 min at 100°C. Samples, including gel-pieces and buffer, were analyzed by SDS-PAGE followed by staining with Coomassie brilliant blue R-250.

Quantification of RPA bound to ssDNA complex by western blotting.

Protein-DNA complexes were eluted from excised gel-piece overnight into 0.5 ml of TE buffer containing 0.1% SDS at room temperature. After reducing the volume to approximately 50 to 100 μl by vacuum concentration, 2 μl of the eluates were spotted on DEAE paper and relative amounts of ssDNA were quantified by measuring the radioactivity using Molecular Dynamics Storm 840 Phospho-Imager and Image-QuaNT software. Western blotting analysis, using 12% SDS-PAGE, was performed with anti-RPA rabbit polyclonal antibody. As standards, the indicated amounts of RPA were also

loaded on the gel. The amount of protein in each sample was determined from the relative intensity of the protein band to the standards, measured using Image-QuaNT software.

Results

Rad51 protein and RPA compete in ssDNA binding.

Previously, we suggested that RPA eliminates DNA secondary structure which impedes presynaptic complex formation by Rad51 protein (7). Since RPA competes with Rad51 protein for binding to ssDNA, we also proposed that bound RPA must be removed from the ssDNA to permit contiguous presynaptic filament formation. Experimentally, the competitive nature of RPA is most clearly manifest by preforming an RPA-ssDNA complex, then introducing Rad51 protein; in this situation, Rad51 protein must displace the RPA from the ssDNA to form a presynaptic complex, and activation of Rad51 protein function is slow (Figure 1A, "RPA-first" process). On the other hand, if Rad51 protein is added to native ssDNA that is free of RPA, it makes a discontinuous presynaptic complex that is interrupted by Rad51 protein-dsDNA regions; addition of RPA stimulates presynaptic complex formation relatively quickly (Figure 1A, “Rad51-first” process). To better understand the nature of presynaptic complex formation in the presence of RPA, we examined the time course of filament formation by each process. The binding of Rad51 protein to ssDNA was measured by monitoring the ATP hydrolysis that accompanies formation of a Rad51 protein-ssDNA complex (Figure 1B), from which the rate of ATP hydrolysis was calculated (Figure 1C). When Rad51 protein was added to a pre-formed RPA-ssDNA complex, ATP hydrolysis did not occur instantly. Rather, the ATP hydrolysis rate increased gradually, and reached a steady-state (2.6 μM/min) approximately 30 min after addition of Rad51 protein (Figure 1B and C, "RPA-first"). Without RPA, the discontinuous Rad51 protein-ssDNA complex showed a slower ATP hydrolysis (1.2 μM/min; Figure 1B, “Rad51-first”) before the

addition of RPA. When RPA was added to this Rad51 protein-ssDNA complex (Figure 1B and C, “Rad51-first”), the ATP hydrolysis rate increased relatively instantly. In the Rad51-first process, 70% of the increase in ATP hydrolysis rate occurred in less than 2 minutes, whereas it took approximately 15 minutes in RPA-first process.

In parallel with the ATPase assays that measured the Rad51 protein-ssDNA binding status, we also measured the DNA-binding status of RPA by fluorescence spectroscopy. RPA has an intrinsic tryptophan fluorescence that is quenched by binding to ssDNA (19). Therefore, the change in fluorescence reflects a change of the RPA-ssDNA binding status. We performed experiments similar to those in Figure 1C, except that we monitored the intrinsic fluorescence of RPA (Figure 1D). As expected, when Rad51 protein was added to an RPA-ssDNA complex, RPA was released from the ssDNA slowly (Figure 1D, "RPA-first"), and reached a plateau level approximately 30 min after addition of Rad51 protein. On the other hand, when RPA was added to a Rad51 protein-ssDNA complex, almost all of the RPA remained unbound throughout the measurement (Figure 1D, "Rad51-first"). For both "RPA-first" and "Rad51-first" processes, the time courses for RPA-release coincided with the time-courses for Rad51 protein-ssDNA complex formation that were measured by monitoring ATP hydrolysis. These results indicate that Rad51 protein displaces RPA from ssDNA upon formation of the presynaptic filament. In addition, the “RPA-first” process is slower than the “Rad51-first” process. These characteristics can explain why RPA has opposite effects on Rad51 protein-mediated functions, which depend on the order of protein-ssDNA complex formation. This behavior of RPA is similar to that of *E. coli* SSB protein with

regard to RecA protein function: displacement of SSB protein by RecA protein is faster for the “RecA-first” than for the “SSB-first” process (23,24).

Displacement of RPA from ssDNA is limited by nucleation of a Rad51 protein-ssDNA complex.

Formation of the RecA nucleoprotein filament is initiated by a rate-limiting nucleation of the protein-DNA complex, followed by cooperative elongation of the filament (25-29). The different rates of RPA displacement in “Rad51-first” and “RPA-first” processes suggest that the rate-limiting step in the RPA-first process for RPA displacement is nucleation of the Rad51-ssDNA complex, rather than elongation of the filament. To confirm this possibility we varied the amount of RPA that was pre-bound to ssDNA, and then Rad51 protein was added to start the displacement reaction (Figure 2). In this experiment, we used poly(dT) instead of pBluescript ssDNA to eliminate any complications arising from DNA secondary structure, since Rad51 protein will bind to both the ssDNA and dsDNA regions. Because the Rad51 protein-dsDNA complex shows much less ATPase activity than the Rad51 protein-ssDNA complex (7), the ATP hydrolysis rate with native ssDNA would not be proportional to the amount of Rad51 protein which bound the DNA. In contrast, by using poly(dT), the ATPase activity will be proportional to formation of the Rad51 protein-ssDNA complex.

When Rad51 protein was added to various subsaturating RPA-poly(dT) complexes (Figure 2A, left four curves), the steady-state rate of ATP hydrolysis was rapidly attained; however, when Rad51 protein was added to saturated RPA-ssDNA complexes (Figure 2A, right four curves), a markedly slower increase in ATP hydrolysis

occurred. Under the latter saturating conditions, the rate of ATP hydrolysis even after 60 minutes incubation was about 30% of that without RPA, and was still increasing slowly. The ATPase activities at 10 min after reaction initiation (Figure 2B) show that concentrations of RPA greater than 0.9 μM precipitously reduced ATP hydrolysis. This concentration of RPA coincides with the concentration required to saturate the poly(dT) (approximately 20 nucleotides per RPA (7)). A slightly lower concentration (0.8 μM) of RPA showed a rather limited reduction of ATP hydrolysis (less than 40%) compared to that of the saturated RPA-poly(dT) complex, even though approximately 90% of ssDNA would be covered by RPA at this concentration. This suggests that the rate-limiting step for displacement at saturating RPA concentrations is the nucleation of Rad51 protein on the RPA-ssDNA complex. Once nucleation occurs, the kinetic curves show that Rad51 protein quickly displaces RPA from ssDNA, presumably by its cooperative assembly along ssDNA. However, in contrast to RecA protein, the distinction between the nucleation and growth phases for Rad51 protein is smaller.

Rad52 protein stimulates Rad51 protein-mediated displacement of RPA from ssDNA.

Rad52 protein stimulates DNA strand exchange by Rad51 protein under conditions where RPA is bound to ssDNA before Rad51 protein (11,12,14). To examine whether this stimulation is due to an accelerated displacement of RPA, we tested the effect of Rad52 protein on both ATP hydrolysis and the displacement of RPA from ssDNA by Rad51 protein. As expected, in the presence of Rad52 protein, the rate of Rad51 protein-dependent ATP hydrolysis increased faster than in the absence of

Rad52 protein (Figure 3A). Similarly, the displacement of RPA from ssDNA by Rad51 protein was accelerated by Rad52 protein (Figure 3B). We also examined whether Rad52 protein itself could displace RPA from ssDNA in the absence of Rad51 protein. When Rad52 protein was added to a RPA-ssDNA complex in the absence of Rad51 protein, no RPA displacement was observed (Figure 3B, "+Rad52 (no Rad51)"). These results show that Rad52 protein alone does not displace RPA from ssDNA but, rather, it facilitates Rad51 protein to do so.

We also analyzed the effect of Rad52 protein on RPA displacement at various concentrations of Rad51 protein (Figure 4). At all concentrations, Rad52 protein stimulated displacement. At the lower concentrations of Rad51 protein (stoichiometric relative to ssDNA concentration, or lower; Figure 3A, and Figure 4A and B, E to G), the stimulation was clear throughout the reaction period; at the higher concentrations of Rad51 protein, stimulation was more modest (Figure 4C and D, E to G). The final rate of ATP hydrolysis, when the Rad51 protein concentration exceeds that needed to saturate the ssDNA, was approximately the same in the presence and the absence of Rad52 protein, supporting the idea that Rad52 protein does not stimulate the ATPase activity of Rad51 protein beyond that of the fully contiguous Rad51 protein-ssDNA complex. These results indicate that the Rad52 protein-mediated stimulation of Rad51 protein function is caused by an acceleration of the loading of Rad51 protein onto an RPA-ssDNA complex with the concomitant release of RPA from the ssDNA.

Rad52 protein-mediated stimulation of presynaptic filament formation is species-specific.

Rad52 protein-mediated stimulation of DNA strand exchange is species-specific (14): Rad52 protein cannot stimulate the reaction either if RPA is replaced by *E. coli* SSB protein, or if Rad51 protein is replaced by *E. coli* RecA protein. To test whether this species-specificity is caused by the specific acceleration of Rad51 protein-ssDNA complex formation by Rad52 protein, we next examined the effect of Rad52 protein on presynaptic complex formation by *E. coli* RecA and SSB proteins. When Rad51 protein was added to SSB-ssDNA complexes, the ATP hydrolysis rate increased gradually to a plateau level in 40 minutes (Figure 5A, "-Rad52"), showing that SSB protein can be displaced by Rad51 protein from ssDNA. Rad52 protein, however, did not affect the time-course of SSB-displacement by Rad51 protein, showing that the stimulation by Rad52 protein is species-specific (Figure 5A, "+Rad52"). When RecA protein was added to an RPA-ssDNA complex, RecA protein also displaced RPA from ssDNA (Figure 5B "-Rad52"). However, Rad52 protein did not stimulate but rather blocked displacement (Figure 5B "+Rad52") . This result is consistent with our previous report which showed that Rad52 protein inhibits DNA strand exchange by RecA protein and RPA (14). Rad52 protein also slowed SSB-displacement by RecA protein (Figure 5C), suggesting that Rad52 protein inhibits either DNA binding or ATP hydrolysis by RecA protein by an unknown mechanism.

We also examined the effect of various Rad52 protein concentrations on presynaptic complex formation, using all combinations of homologous and heterologous proteins: Experiments such as those shown in Figure 5A to C were performed, and the relative ATPase activity at 5 minutes after addition of Rad51 protein was plotted against the concentration of Rad52 protein (Figure 6), because both stimulation and inhibition

were clear at this early stage of the displacement. Rad52 protein stimulated the ATP hydrolysis activity of Rad51 protein only when RPA was used. The optimum Rad52 protein concentration for the stimulation (approximately 0.5 μM) was similar to the concentration of RPA which was bound to ssDNA. This suggests that a stoichiometric co-complex of Rad52 protein and RPA on ssDNA is involved in the displacement. The displacement of SSB protein by Rad51 protein was not affected at any concentration of Rad52 protein. RecA-mediated displacement of both RPA and SSB protein was inhibited by Rad52 protein in a concentration-dependent manner. These results confirm the need for cognate, species-specific interactions in the Rad52 protein-mediated stimulation of presynaptic complex formation.

Detection of a Rad52 protein-RPA-ssDNA co-complex.

In the experiments presented so far, we analyzed both ATP hydrolysis by Rad51 protein to follow its binding to ssDNA, and the fluorescence of RPA to follow its binding to DNA. Although each method detects the respective status of which protein was bound to ssDNA, neither provides any information regarding the interaction of Rad52 protein with the RPA-ssDNA complex. Because T4 phage UvsY protein and *E. coli* RecO protein, which are functional homologues of Rad52 protein, can form a co-complex with the gp32-ssDNA complex and the SSB protein-ssDNA complex, respectively (30,31), it was of special interest to test whether Rad52 protein could also produce a co-complex with the RPA-ssDNA complex. Therefore, we examined the binding of Rad52 protein to RPA-ssDNA complexes using a gel mobility-shift assay.

Incubation of RPA and 100-mer ssDNA produced an RPA-ssDNA complex with a reduced electrophoretic mobility (Figure 7A); titration with RPA showed that 0.7 μM is sufficient to saturate the 10 μM of ssDNA. Similarly, titration of the ssDNA with Rad52 protein also produced Rad52 protein-ssDNA complexes which either entered the gel or stacked in the wells (Figure 7B). These results are consistent with previous reports regarding the binding of RPA and Rad52 protein to ssDNA (10,19). Interestingly, adding an increasing amount of Rad52 protein to the saturated RPA-ssDNA complex changed the mobility of the complex to one that is stacked in the wells (Figure 7C, indicated as "super-shifted complex"). To examine which proteins are components of the super-shifted complex, the bands corresponding to the "super-shifted" complex were excised and analyzed by SDS-PAGE. To enable direct comparison of the amounts of the proteins present in each complex, we normalized the amount of protein present to the amount of ssDNA present, which was measured from radioactivity of the ssDNA. Compared to the control RPA-ssDNA complex (Figure 7D lane 6), the super-shifted complexes (lanes 7 to 9) contained similar amounts of RPA per ssDNA molecule, despite the presence of increasing amounts of Rad52 protein (Figure 7D and E). Importantly, these complexes also contained Rad52 protein, the amount of which depended on the concentration of Rad52 protein added to the RPA-ssDNA complex. These results indicate that Rad52 protein and RPA can form a co-complex that is bound to ssDNA. This complex is not just a mixture of RPA-ssDNA and Rad52-ssDNA complexes, because the amount of RPA in the co-complex remains constant with increasing amount of Rad52 protein. To exclude the possibility of a DNA-independent aggregation of Rad52 protein or of RPA in the mobility-shift experiments, we performed

the same experiment as for lane 9 of Figure 7D, but in the absence of ssDNA. The gel piece corresponding to the co-complex contained an undetectable amount of RPA or Rad52 protein in this control (Figure 7D, lane 10).

RPA is absent from the presynaptic filament.

Our fluorescence experiments indicated only the ssDNA-binding status of RPA (Figure 1D and 3B). We could not distinguish whether RPA was free in solution or whether it remained bound to the Rad51 protein-ssDNA complex *via* protein-protein interactions after being removed from ssDNA. To address this issue, we asked whether Rad51 protein and RPA could form a complex. Initially, we incubated various amounts of Rad51 protein with the 100-mer ssDNA in the absence of RPA using the standard gel mobility-shift protocol. Rad51 protein produced only a faint shift under these conditions (Figure 8A). However, when ATP, NaCl, and magnesium acetate were added to both the gel and the electrophoresis buffer, the Rad51 protein-ssDNA complex was observed more clearly, as a species that stacked in the sample well (Figure 8B; see Experimental Procedures for details). This finding suggested that the Rad51 protein-ssDNA complex was unstable without those components, and that it dissociated during electrophoresis. Therefore, electrophoresis was performed using the latter conditions. When an increasing amount of Rad51 protein was added to a saturated RPA-ssDNA complex, the mobility of the ssDNA changed to that of the Rad51 protein-ssDNA complex (Figure 8C lanes 1 to 6). To examine whether RPA was present within this new complex, we measured the amount of RPA in the complexes (Figure 8D and E). Consistent with our RPA-displacement interpretation, the new complex contained a lower amount of RPA

(1/5 or less) than the control RPA-ssDNA complex (compare lanes 6 and 7 of D, and lanes 5 and 7 of E). This result confirms our conclusion that Rad51 protein displaces RPA from ssDNA and, furthermore, that RPA is not forming a stable interaction with the Rad51 protein-ssDNA presynaptic complex after having been displaced.

Rad52 protein (0.7 μM) did not affect the formation of the new complex (Figure 8C, lanes 7 to 12). This was not surprising because we did not detect Rad52 protein-mediated stimulation of DNA-pairing with synthetic oligonucleotides and because RPA-displacement measured by ATPase activity showed that the displacement occurred too quickly on such short ssDNA to permit detectable stimulation by Rad52 protein (data not shown). Nevertheless, the amount of RPA also decreased in the Rad51 protein-ssDNA complex (Figure 8D and E, compare lanes 6 and 8), showing that the majority of RPA molecules were released from the presynaptic complex even in the presence of Rad52 protein, which can interact with both Rad51 protein and RPA. Finally, we found Rad51 protein in the gel pieces corresponding to Rad51 protein-ssDNA complex (Figure 8D, lanes 7 to 9); however, the majority of this signal is due to DNA-independent aggregation of Rad51 protein under these gel electrophoresis conditions, because negative control experiments without ssDNA also detected a similar amount of Rad51 protein (lanes 10 and 11). Therefore, we could not quantify the amount of Rad51 protein in the complexes formed with ssDNA.

Discussion

RPA can greatly stimulate Rad51 protein-mediated DNA strand exchange, provided that RPA is added to a preformed complex of Rad51 protein and native ssDNA. One possible explanation for this stimulation is that RPA forms a co-complex with the Rad51 protein-ssDNA complex that is more active in DNA strand exchange. However, the results in this and in our previous work (7) suggest otherwise; instead, they indicate that RPA and Rad51 protein compete with each other for the same ssDNA binding sites. In this paper, we present direct evidence showing that RPA is released from ssDNA by Rad51 protein, and that this release correlates exactly with formation of the Rad51 protein-ssDNA complex. This means that the presynaptic complex, which is assembled in the presence of RPA, is simply a complex of Rad51 protein and ssDNA rather than a co-complex of Rad51-ssDNA-RPA. We also showed that the time course for presynaptic complex formation depends on the order that the proteins are bound to ssDNA. The displacement of RPA by Rad51 protein from a pre-formed RPA-ssDNA complex takes a relatively long period of time (20 to 30 minutes), but RPA acts on Rad51 protein-ssDNA complexes instantly, without the detection of a significant level of RPA-ssDNA complex as an intermediate. In addition, the experiments which vary the occupancy of ssDNA by RPA (Figure 2) suggest that the rate-limiting step of the displacement reaction is the nucleation of Rad51 protein onto ssDNA. Once nucleation occurs, extensive displacement of RPA occurs by growth of the Rad51 filament along ssDNA. These characteristics are similar to the behavior of *E. coli* RecA and SSB proteins, whereby SSB protein stimulates RecA presynaptic filament formation by a related mechanism (23,24). We could not detect interaction of RPA with the filament at

this stage, even in the presence of Rad52 protein. Rad52 protein may be interacting with the Rad51 presynaptic complex *via* a protein-protein interaction, but such a hypothetical complex has no effect on the DNA pairing activity, since Rad52 protein has no stimulatory effect on the pre-formed Rad51 presynaptic complex (12,14,32).

Based on the observations in this paper and others, we conclude that Rad51 protein and RPA compete for binding to ssDNA. Although this competition can have a detrimental effect, when the ssDNA has secondary structure, RPA is needed to melt the DNA secondary structure. In the absence of RPA, Rad51 protein binds the duplex regions and inhibits DNA strand exchange. RPA is needed to prevent this binding, but then Rad51 protein nevertheless displaces RPA from ssDNA. When the ssDNA is fully saturated with RPA, nucleation of Rad51-ssDNA binding is a relatively inefficient process. However, once Rad51 protein nucleates on ssDNA, filament extension along ssDNA creates a contiguous Rad51-filament on the DNA that concomitantly displaces the bound RPA. The function of Rad52 protein, therefore, is to help Rad51 protein displace RPA from ssDNA since Rad52 protein alone cannot displace RPA from ssDNA.

Our results also show that Rad52 protein and RPA form a co-complex on ssDNA. This function of yeast Rad52 protein is similar to that of T4 phage UvsY protein and *E. coli* RecO (or RecOR) protein (see (33), for a review). Each of these “recombination mediator” proteins recruits its DNA strand exchange proteins to ssDNA to overcome the inhibitory effect of ssDNA binding proteins, but none of them can displace ssDNA-binding proteins by themselves. Instead, each mediator protein specifically interacts with its cognate ssDNA-binding protein, an interaction that is a universal property of the

DNA strand exchange mediators. Since RPA is a relatively abundant protein in the cell, it is reasonable to expect that ssDNA produced *in vivo* is first coated with RPA. In fact, cytological observations confirm the temporal order of protein appearance that we have elaborated *in vitro* (34). These analyses also showed that RPA and Rad52 protein co-localize in subnuclear foci at double-strand breaks, as an early step of recombination. This co-localization may involve the co-complex formation of RPA and Rad52 protein on ssDNA which is produced by processing of the DNA breaks, prior to their displacement by Rad51 protein.

Since Rad52 protein by itself cannot displace RPA from ssDNA, there are several possible mechanisms by which Rad52 protein could facilitate assembly of Rad51 protein on ssDNA. Perhaps the simplest one is that Rad52 protein serves as a nucleus for Rad51 protein filament assembly, *via* an interaction with the RPA-ssDNA complex. Because the rate-limiting step for RPA-displacement is the nucleation step of Rad51 protein filament assembly, facilitation of nucleation accelerates the displacement process. Similar mechanisms were proposed for *E. coli* RecO protein (31,35), and for T4 UvsY protein (33,36). Alternatively, Rad52 protein might increase the elongation phase of Rad51 filament assembly. However, this possibility is less likely, because elongation of Rad51 filament is not strongly inhibited by RPA. Finally, a third possibility relies on protein-protein interactions that exist between Rad52 protein and RPA, and between Rad52 and Rad51 protein: in principle, these three proteins could form a transient Rad51-Rad52-RPA-ssDNA nucleoprotein co-complex as an intermediate. In the T4 phage system, a three protein and DNA co-complex was proposed as an intermediate (30), but recent studies showed that the gp32-ssDNA interaction is

destabilized by interaction with UvsY protein, to facilitate loading of UvsX protein onto ssDNA (37). So far, however, we have not detected any destabilization of the RPA-ssDNA complex by Rad52 protein (unpublished observations). In this paper, we detected a Rad52-RPA-ssDNA co-complex *in vitro.* Since the amount of Rad52 protein which is needed for the displacement of RPA is approximately the same as the amount of RPA which is bound to ssDNA, the active species of the displacement may be a stoichiometric complex of Rad52 protein and RPA on ssDNA (Figure 9b). In addition, both Rad52 protein and UvsY protein form ring-like structure (heptamer for Rad52 protein and hexamer for UvsY), and this multimerization is required for UvsY function (11,38,39). Therefore, for the reasons outlined above, we favor the facilitated nucleation model as depicted in Figure 9.

References

1. Shinohara, A., Ogawa, H., and Ogawa, T. (1992) *Cell* **69**, 457-470
2. Aboussekhra, A., Chanet, R., Adjiri, A., and Fabre, F. (1992) *Mol Cell Biol* **12**, 3224-3234
3. Basile, G., Aker, M., and Mortimer, R. K. (1992) *Mol Cell Biol* **12**, 3235-3246
4. Bianco, P. R., Tracy, R. B., and Kowalczykowski, S. C. (1998) *Front Biosci* **3**, D570-D603.
5. Sung, P. (1994) *Science* **265**, 1241-1243
6. Sung, P., and Robberson, D. L. (1995) *Cell* **82**, 453-461
7. Sugiyama, T., Zaitseva, E. M., and Kowalczykowski, S. C. (1997) *J Biol Chem* **272**, 7940-7945
8. Heyer, W.-D., Rao, M. R. S., Erdile, L. F., Kelly, T. J., and Kolodner, R. D. (1990) *EMBO J.* **9**, 2321-2329
9. Brill, S. J., and Stillman, B. (1991) *Genes Dev* **5**, 1589-1600
10. Mortensen, U. H., Bendixen, C., Sunjevaric, I., and Rothstein, R. (1996) *Proc Natl Acad Sci U S A* **93**, 10729-10734
11. Shinohara, A., Shinohara, M., Ohta, T., Matsuda, S., and Ogawa, T. (1998) *Genes Cells* **3**, 145-156
12. Sung, P. (1997) *J Biol Chem* **272**, 28194-28197
13. Shinohara, A., and Ogawa, T. (1998) *Nature* **391**, 404-407
14. New, J. H., Sugiyama, T., Zaitseva, E., and Kowalczykowski, S. C. (1998) *Nature* **391**, 407-410

15. Benson, F. E., Baumann, P., and West, S. C. (1998) *Nature* **391**, 401-404

16. Ivanov, E. L., Sugawara, N., Fishman-Lobell, J., and Haber, J. E. (1996) *Genetics* **142**, 693-704

17. Sugiyama, T., New, J. H., and Kowalczykowski, S. C. (1998) *Proc Natl Acad Sci U S A* **95**, 6049-6054

18. Ausubel, F. M. (1987) *Current protocols in molecular biology*, Published by Greene Pub. Associates and Wiley-Interscience : J. Wiley, New York

19. Alani, E., Thresher, R., Griffith, J. D., and Kolodner, R. D. (1992) *J Mol Biol* **227**, 54-71

20. Kowalczykowski, S. C., Bear, D. G., and von Hippel, P. H. (1981) in *The Enzymes* (Boyer, P. D., ed), pp. 373-442, Academic Press, New York

21. LeBowitz, J. (1985), Johns Hopkins University, Baltimore, MD

22. Kreuzer, K. N., and Jongeneel, C. V. (1983) *Methods Enzymol.* **100**, 144-160

23. Kowalczykowski, S. C., Clow, J. C., Somani, R., and Varghese, A. (1987) *J. Mol. Biol.* **193**, 81-95

24. Kowalczykowski, S. C., and Krupp, R. A. (1987) *J. Mol. Biol.* **193**, 97-113

25. Kowalczykowski, S. C., Clow, J., and Krupp, R. A. (1987) *Proc. Natl. Acad. Sci. USA* **84**, 3127-3131

26. Chabbert, M., Cazenave, C., and Helene, C. (1987) *Biochemistry* **26**, 2218-2225

27. Pugh, B. F., and Cox, M. M. (1987) *J. Biol. Chem.* **262**, 1326-1336

28. Pugh, B. F., and Cox, M. M. (1988) *J. Mol. Biol.* **203**, 479-493

29. Kowalczykowski, S. C. (1991) *Annu Rev Biophys Biophys Chem* **20**, 539-575

30. Hashimoto, K., and Yonesaki, T. (1991) *J Biol Chem* **266**, 4883-4888

31. Umezu, K., and Kolodner, R. D. (1994) *J Biol Chem* **269**, 30005-30013

32. Song, B., and Sung, P. (2000) *J Biol Chem* **275**, 15895-15904

33. Beernink, H. T. H., and Morrical, S. W. (1999) *Trends in Biochemical Sciences* **24**, 369-410

34. Gasior, S. L., Wong, A. K., Kora, Y., Shinohara, A., and Bishop, D. K. (1998) *Genes Dev* **12**, 2208-2221

35. Shan, Q., Bork, J. M., Webb, B. L., Inman, R. B., and Cox, M. M. (1997) *J Mol Biol* **265**, 519-540

36. Beernink, H. T., and Morrical, S. W. (1998) *Biochemistry* **37**, 5673-5681

37. Sweezy, M. A., and Morrical, S. W. (1999) *Biochemistry* **38**, 936-944

38. Stasiak, A. Z., Larquet, E., Stasiak, A., Muller, S., Engel, A., Van Dyck, E., West, S. C., and Egelman, E. H. (2000) *Curr Biol* **10**, 337-340

39. Ando, R. A., and Morrical, S. W. (1999) *Biochemistry* **38**, 16589-16598

Acknowledgement

We thank Dr. Richard Kolodner for the RPA overproducing strain, and Dr. Wolf-D. Heyer for anti-RPA antibody, Piero Bianco, Mark Dillingham, Naofumi Handa, Cynthia Haseltine, Noriko Kantake, Alex Mazin, Katsumi Morimatsu, Jim New, and Yun Wu for comments on the manuscript. This work was supported by Grants AI-18987 and GM-62653 from the National Institutes of Health and by RG63 from the Human Frontier Science Program to S.C.K.

Figure legends

Figure 1. RPA displacement from ssDNA coincides with presynaptic complex formation by Rad51 protein.

A. Schematic drawing of presynaptic complex formation where either RPA ("RPA-first") or Rad51 protein ("Rad51-first") is pre-bound to ssDNA. B. ATP hydrolysis measures presynaptic complex formation. Rad51 protein (5 μM) and RPA (1 μM) were added to pBluescript SK- ssDNA (10 μM) as indicated. C and D. Comparison of the development of Rad51 protein-dependent ATPase activity (*i.e.*, presynaptic complex formation) with the displacement of RPA from ssDNA. Time courses for the ATP hydrolysis rate (C) were calculated as the first derivative of the data in B. Displacement of RPA from ssDNA (D) was monitored as described in the Experimental Procedures. For both C and D, the reactions were started by adding Rad51 protein to the RPA-ssDNA complex (△), or by adding RPA to a preformed Rad51 protein-ssDNA complex (●). Dashed line in C indicates the ATP hydrolysis rate of the Rad51-first reaction before addition of RPA. The RPA fluorescence is quenched 41% by binding to ssDNA under these conditions in the absence of Rad51 protein, and this quenched level is defined as 0% RPA released.

Figure 2. Saturation of ssDNA with RPA limits the ability of Rad51 protein to displace RPA.

A. ATP hydrolysis was monitored in "RPA-first" experiments like those in Figure 1B, using 0, 0.27, 0.53, 0.8, 0.9, 1.2, 1.7, or 2.7 μM of RPA (lines from left to right; 1.7 and 2.7 μM curves are overlaid), which were preincubated with 13.7 μM of poly(dT). Rad51

protein (5 μM) was added to start the reactions. B. The ATP hydrolysis rate after 10 minutes was plotted against the concentration of RPA.

Figure 3. Rad52 protein helps Rad51 protein to displace RPA from ssDNA.

Time-courses of ATPase activity (A) and the release of RPA from ssDNA (B) were monitored using the RPA-ssDNA complex as a starting substrate. The reactions were started by addition of Rad51 protein (5 μM) to a preformed complex of RPA (1 μM) and pBluescript SK- ssDNA (10 μM). Where indicated ("+Rad52"), Rad52 protein (1 μM) was added 20 to 30 seconds after addition of Rad51 protein. For the "+Rad52 (no Rad51)" reaction, Rad52 protein was added to a preformed RPA-ssDNA complexes in the absence of Rad51 protein. The fluorescence of Rad51 and Rad52 proteins was subtracted in the fluorescence analyses.

Figure 4. Rad52 protein facilitates both the rate and extent of RPA-displacement from ssDNA.

A to D. ATP hydrolysis was measured as in Figure 3A, using 2 μM (A), 3 μM (B), 7 μM (C), and 10 μM (D) of Rad51 protein in the presence (- △ -) or the absence (- ● -) of Rad52 protein (1 μM). E to G. ATP hydrolysis rate after 2 min (C), 5 min (D), and 40 min (E), in the presence (- △ -) or the absence (- ● -) of Rad52 protein, plotted against the Rad51 protein concentration.

Figure 5. The RPA-displacement function of Rad52 protein is species-specific.

Presynaptic complex formation by either Rad51 protein or RecA protein, in the presence of either *E. coli* or yeast ssDNA-binding protein, was examined by measuring ATP hydrolysis. A to C. The ATP hydrolysis reactions were started by adding Rad51 (5 μM; A) or RecA protein (3.3 μM; B and C) to pBluescript SK- ssDNA (10 μM) which was pre-bound with 1 μM of RPA (B) or 1.2 μM of SSB protein (A and C). Rad52 protein was added immediately after the reaction start (at approximately 15 sec). For the RecA protein reactions, the reaction conditions were the same as for the Rad51 protein reactions except that KCl was omitted, and 1.5 mM of phosphoenolpyruvate, 15 U/ml of pyruvate kinase, and 15 U/ml of lactate dehydrogenase were added. Open triangles with dashed lines and filled circles with solid lines represent the reactions with and without 1 μM Rad52 protein, respectively.

Figure 6. Rad52 protein facilitates ssDNA binding protein-displacement only by the cognate DNA strand exchange protein at all concentrations.

Experiments, as in Figure 5, were performed in the presence of various amounts of Rad52 protein, and the ATP hydrolysis rates at 5 min after addition of Rad51 protein were plotted against the concentration of Rad52 protein. The ATP hydrolysis rates are shown as relative to the rate obtained without Rad52 protein. The reactions with Rad51 protein and RPA (- ○ -), Rad51 protein and SSB protein (- ■ -), RecA protein and RPA (- ▲ -), and RecA protein and SSB (- ∇ -) are shown.

Figure 7. Formation of a RPA and Rad52 protein co-complex bound to ssDNA.

A and B. The indicated amounts of RPA (A) and Rad52 protein (B) were incubated with ^{32}P-labeled 100-mer ssDNA (10 μM) under the standard conditions without ATP, and samples were analyzed by "conventional" electrophoresis (see Experimental Procedures for details). C. RPA-ssDNA complexes were first formed by incubating ssDNA with 0.7 μM of RPA, and then various amounts of Rad52 protein were added to produce ssDNA-RPA-Rad52 protein co-complex. The reaction did not contain ATP, since it had no effect on the co-complex formation (data not shown). Samples were analyzed by "conventional" electrophoresis. D. Analysis of the Rad52 protein-RPA-ssDNA co-complex. The gel-mobility-shift experiments as shown in lane 1 of C (RPA-ssDNA complex, lane 6) and lanes 4, 6, and 7 of C ("super-shift" complex, lane 7 to 9), and lane 7 of B (Rad52-ssDNA complex, lane 11) were done in three-fold larger volume, and the super-shifted complexes containing an equivalent amount of ssDNA were analyzed by SDS-PAGE followed by staining with Coomassie brilliant blue R-250. Lane 10 is the same as lane 9 except that the gel-shift experiment had no ssDNA and twice the amount of gel piece was loaded on the gel. Lanes 1 to 5 are standards showing 0.03 μg, 0.1 μg, 0.3 μg, 1 μg, and 3 μg of RPA and Rad52 protein, respectively. Lane M is pre-stained markers, showing 116 kDa, 78.0 kDa, 49.3 kDa, and 34.7 kDa. E. Relative molar amount of RPA and Rad52 protein in RPA-ssDNA complex, Rad52-RPA-ssDNA co-complexes and Rad52 protein-ssDNA complex were calculated based on D. The amount of RPA in RPA-ssDNA complex was defined as 1.

Figure 8. Binding of Rad51 protein to ssDNA and displacement of RPA monitored by gel mobility-shift assay

A. The indicated amounts of Rad51 protein were incubated with ^{32}P-labeled 100-mer ssDNA (10 μM) under standard conditions with ATP, and the samples were analyzed by "conventional" electrophoresis. B. The same Rad51 protein-titration experiment as A was done except that the samples were analyzed by electrophoresis in the presence of ATP and Mg^{++} (see Experimental Procedures for details). C. RPA-ssDNA complexes were first formed by incubating ssDNA with 0.7 μM of RPA for 10 min in the buffer containing ATP, and then with (lanes 7 to 12) or without (lanes 1 to 6) 0.7 μM of Rad52 protein for 10 min; finally the indicated amounts of Rad51 protein were added and incubated for 15 min. Samples were analyzed by electrophoresis in the presence of ATP and Mg^{++}. D. Analysis of the Rad51 protein-ssDNA complex after displacement. The same gel-mobility-shift experiments as shown B and C were done in three-fold larger volume, and the RPA-ssDNA complex which was recovered from lane 1 of C (lane 6), the Rad51 protein-ssDNA complexes which were recovered from lanes 6 and 12 of C (lanes 7 and 8) and from lane 7 of B (lane 9), each containing an equivalent amount of ssDNA, were analyzed by SDS-PAGE followed by staining with Coomassie brilliant blue R-250. Lanes 10 and 11 are the same as lanes 7 and 8, respectively, except that the gel-shift experiments had no DNA, and that twice the amount of gel pieces were loaded on the gel. Lanes 1 to 5 are standards showing 0.03 μg, 0.1 μg, 0.3 μg, 1 μg, and 3 μg of RPA, Rad51 protein, and Rad52 protein. Lane M is pre-stained markers, showing 116 kDa, 78.0 kDa, 49.3 kDa, and 34.7 kDa. E. RPA-ssDNA complex in lane 1 of C (lane 5), RPA-ssDNA complex in lane 7 of C (lane 6), Rad51 protein-ssDNA complex in lane 6 of C (lane 7), and Rad51 protein-ssDNA complex in lane 12 of C (lane 8) were analyzed by western blotting using anti-RPA. The amount of

sample was normalized by DNA content. Lanes 1 to 4 are standards showing 5 ng, 10 ng, 20 ng and 50 ng of RPA. Lane M indicate markers.

Figure 9. A model for presynaptic complex formation by Rad51 and Rad52 proteins and RPA.

Rad52 protein binds to RPA-ssDNA complex (a) to form a Rad52-RPA-ssDNA nucleoprotein co-complex (b). This co-complex facilitates the nucleation of Rad51 protein onto ssDNA. The ring-form of Rad52 protein may be involved in this step (c). Nucleation is followed by rapid elongation of the Rad51 filament to form a contiguous Rad51-ssDNA presynaptic complex (d).

Suggested location of Figures

Figure 1: in the first section of Results

Figure 2: in the second section of Results

Figure 3: in the third section of Results

Figure 4: in the third section of Results

Figure 5: in the fourth section of Results

Figure 6: in the fourth section of Results

Figure 7: in the fifth section of Results

Figure 8: in the sixth section of Results

Figure 9: in Discussion

Fig. 1
Sugiyama and Kowalczykowski

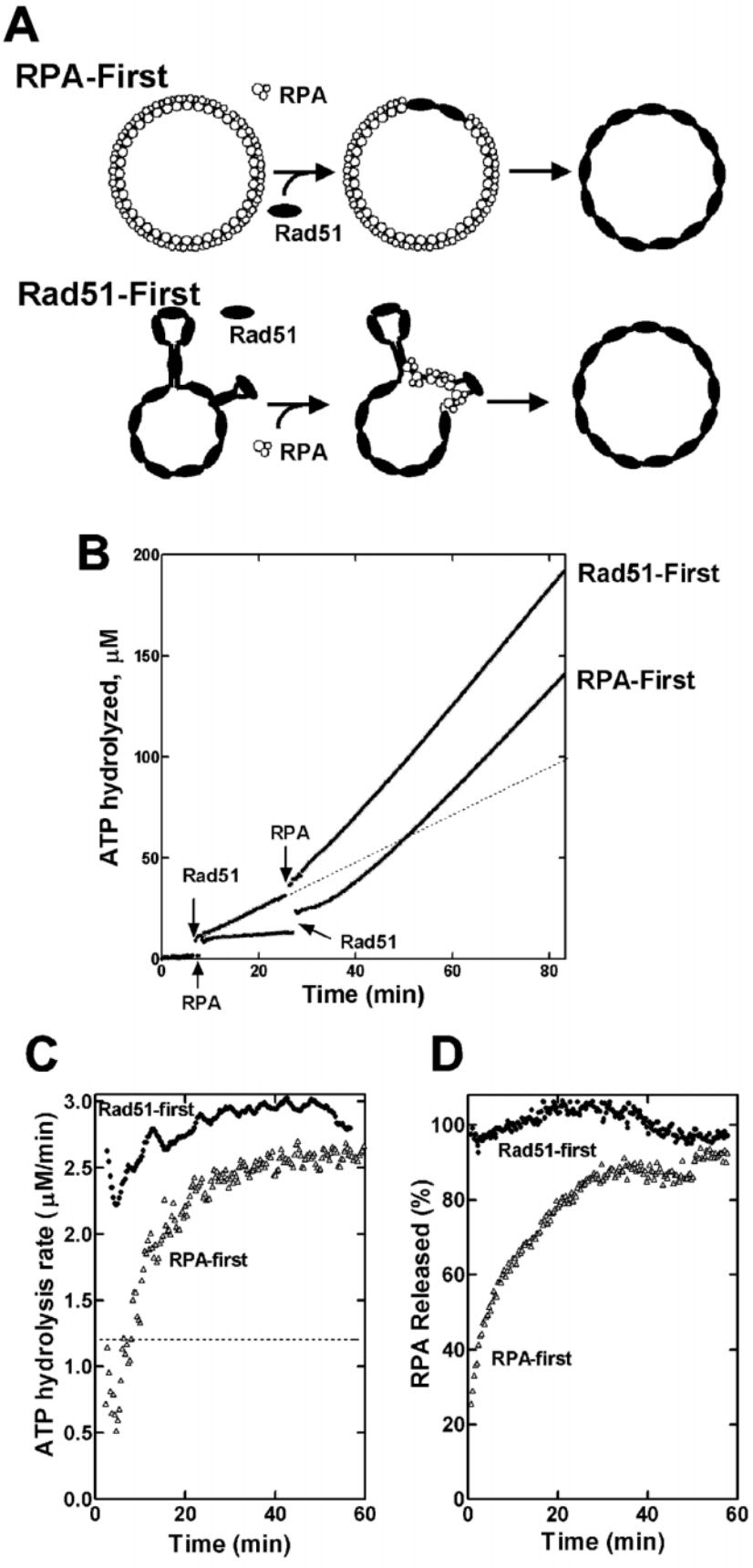

Fig.2
Sugiyama & Kowalczykowski

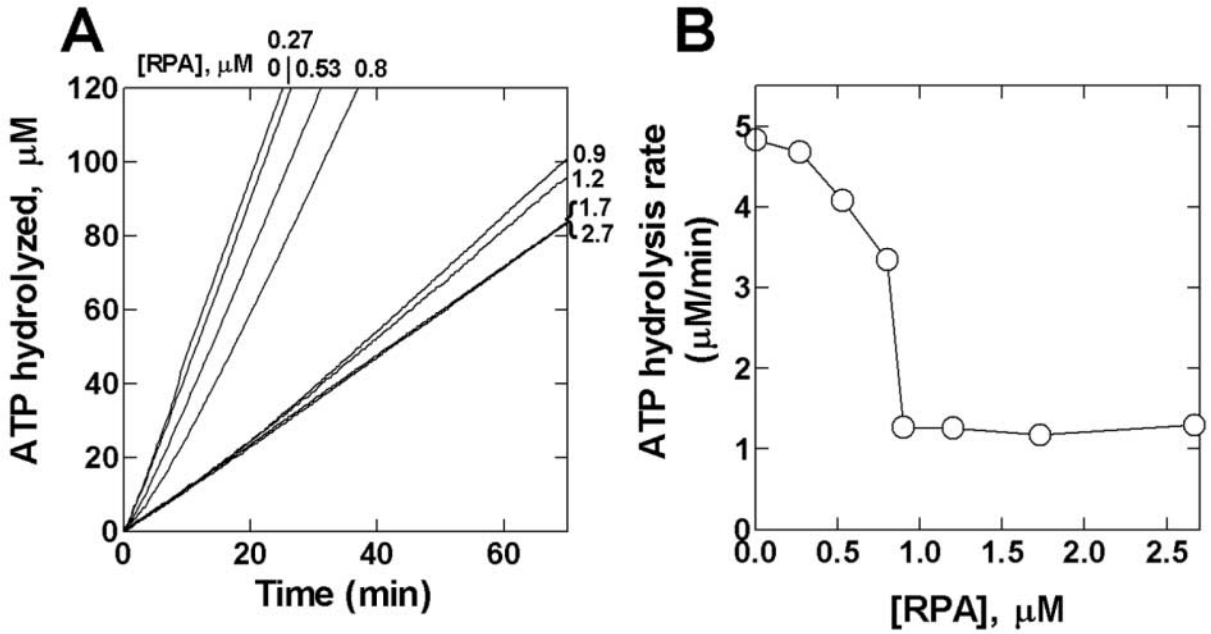

Fig. 3
Sugiyama & Kowaczykowski

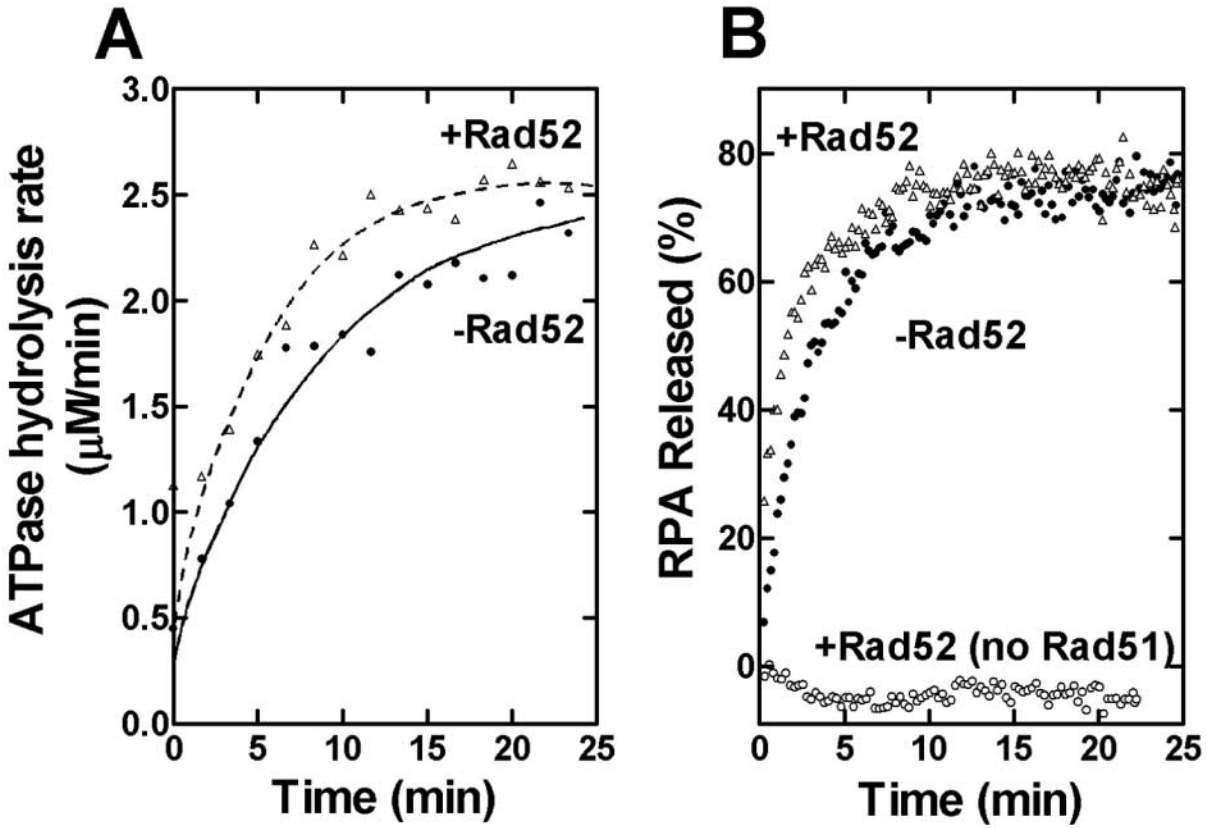

Fig. 4
Sugiyama and Kowalczykowski

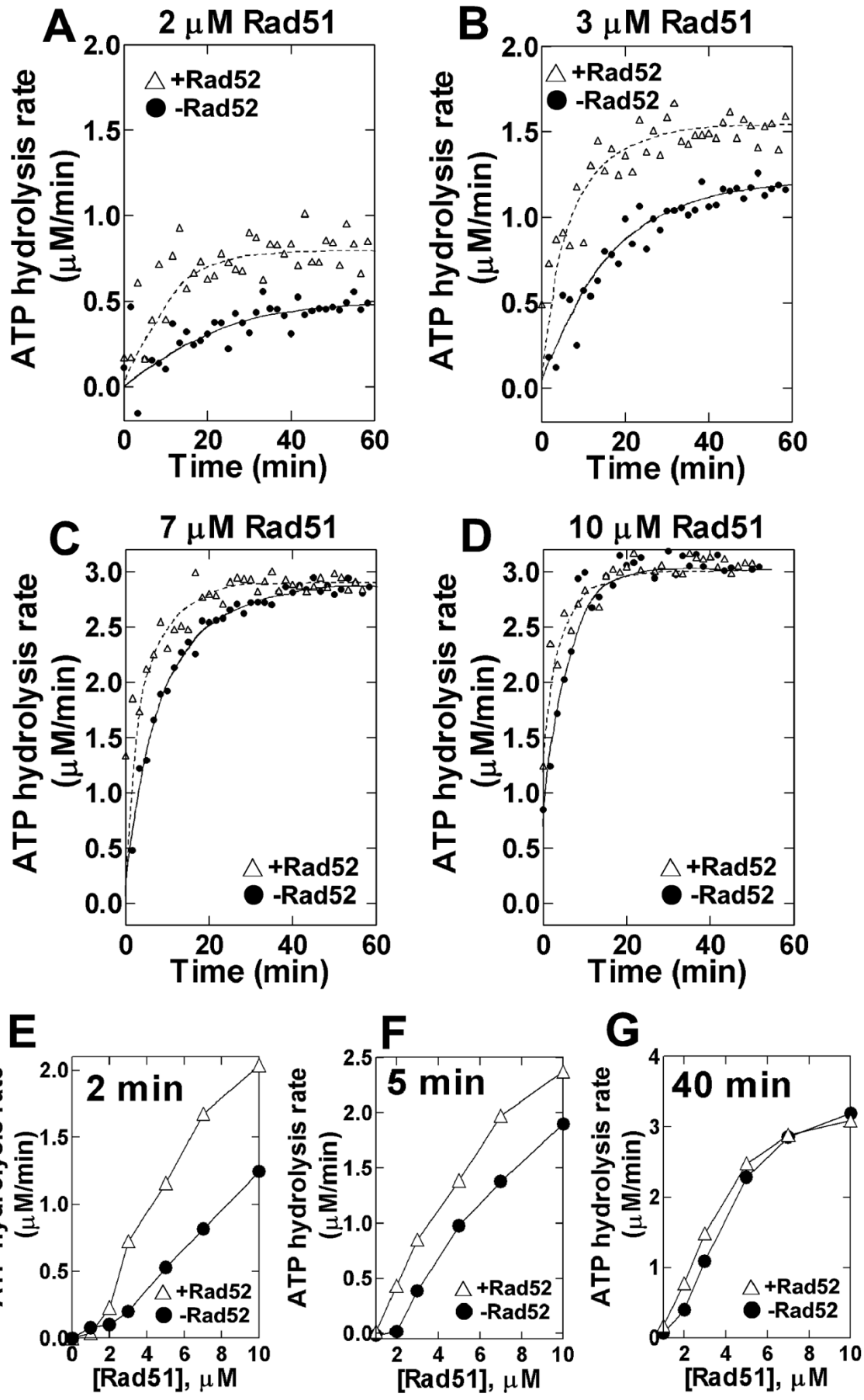

Fig. 5
Sugiyama &
Kowalczykowski

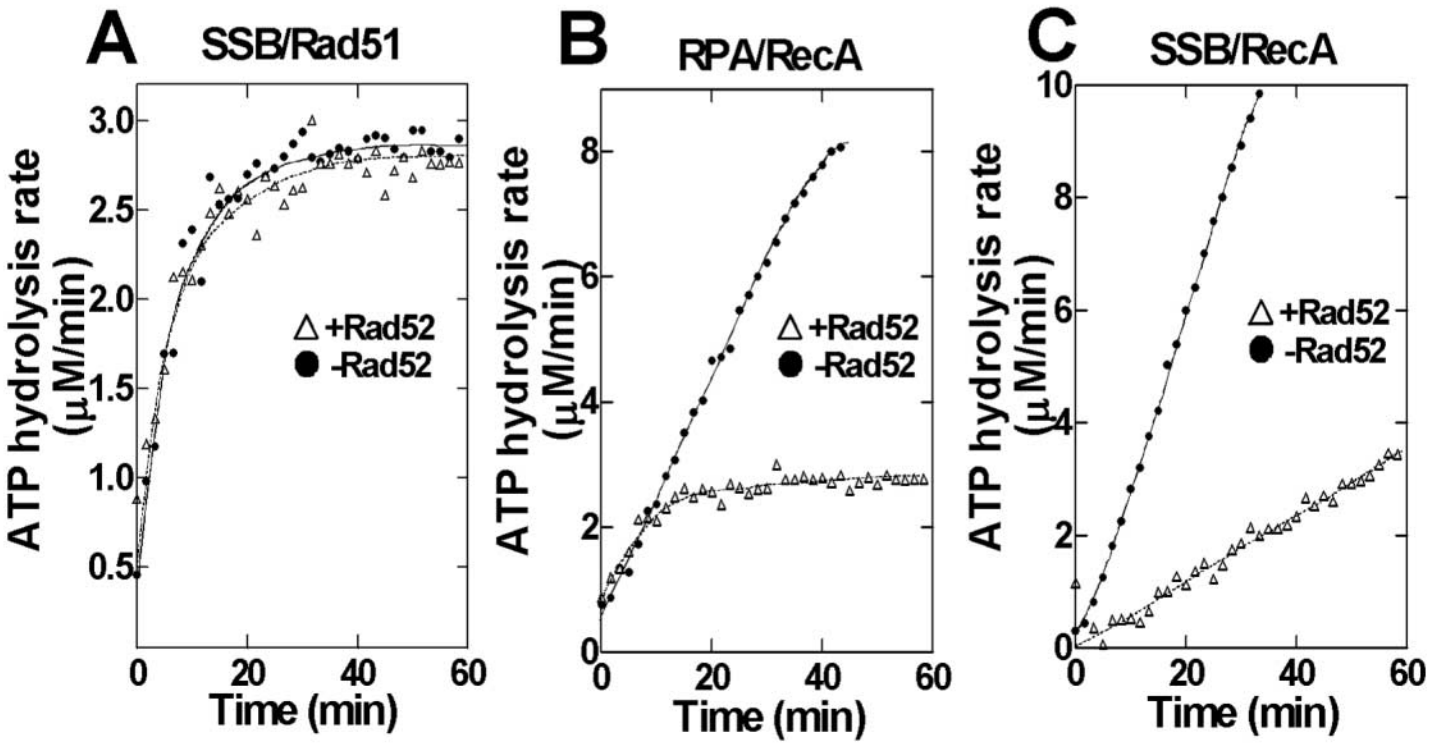

Fig. 6
Sugiyama &
Kowalczykowski

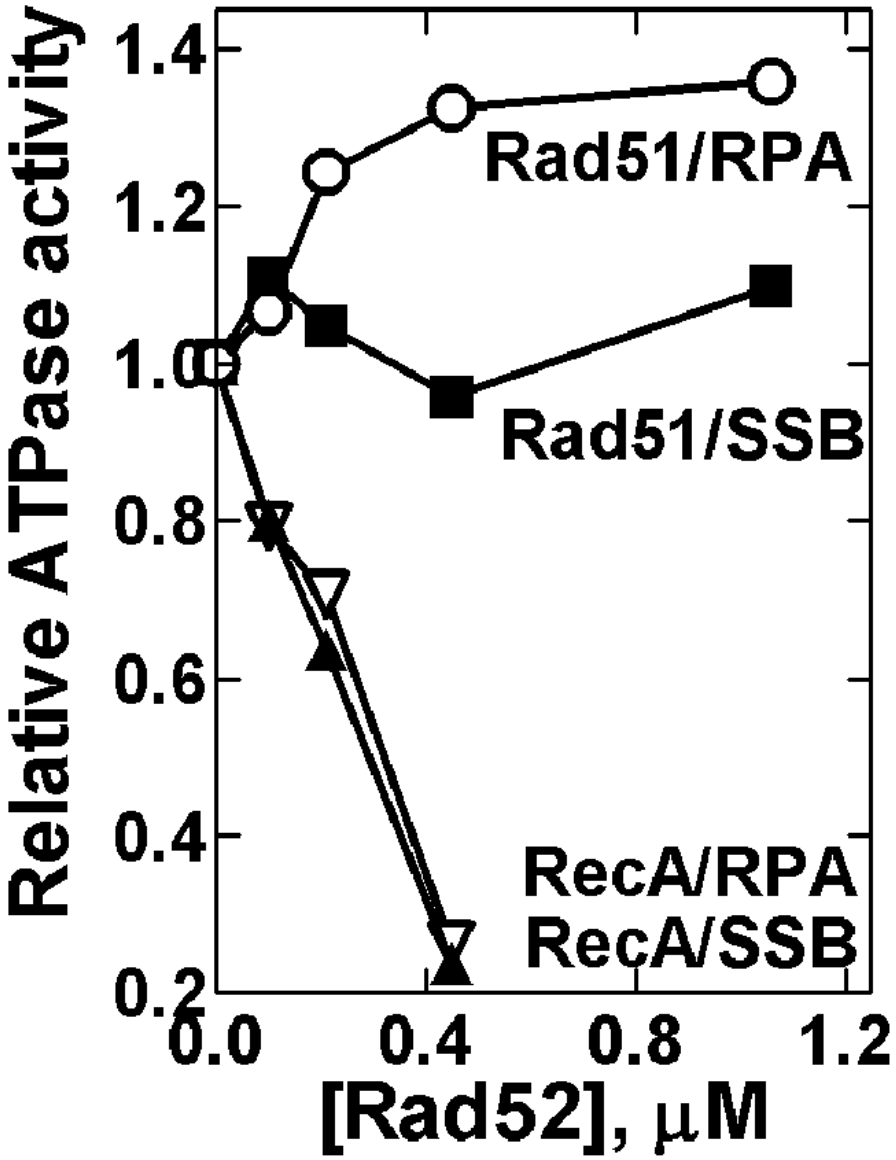

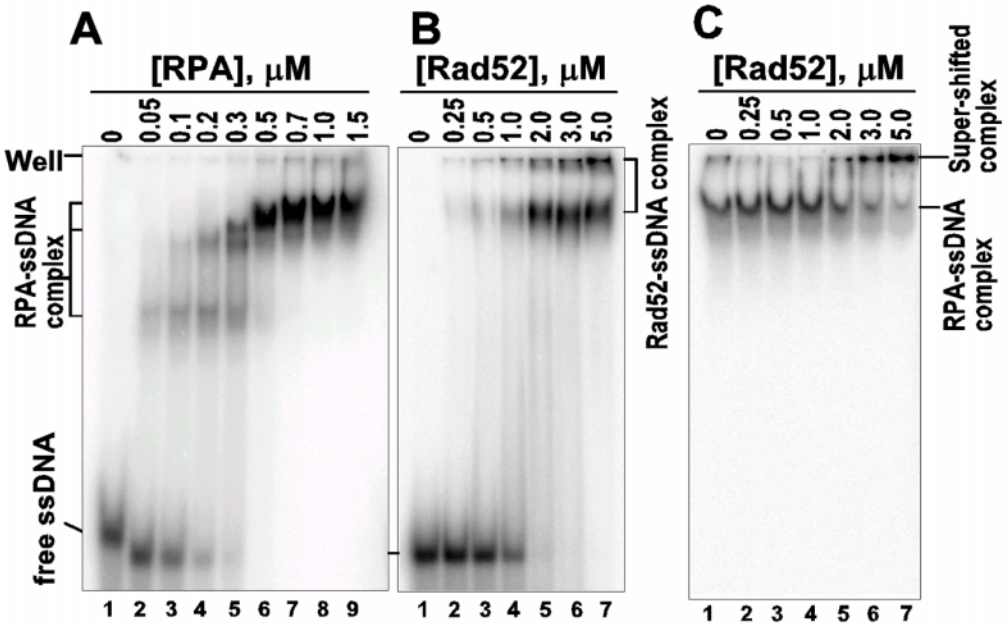
A
[RPA], μM
0
0.05
0.1
0.2
0.3
0.5
0.7
1.0
1.5
Well
RPA-ssDNA complex
free ssDNA
1 2 3 4 5 6 7 8 9
B
[Rad52], μM
0
0.25
0.5
1.0
2.0
3.0
5.0
Rad52-ssDNA complex
1 2 3 4 5 6 7
C
[Rad52], μM
0
0.25
0.5
1.0
2.0
3.0
5.0
Super-shifted complex
RPA-ssDNA complex
1 2 3 4 5 6 7

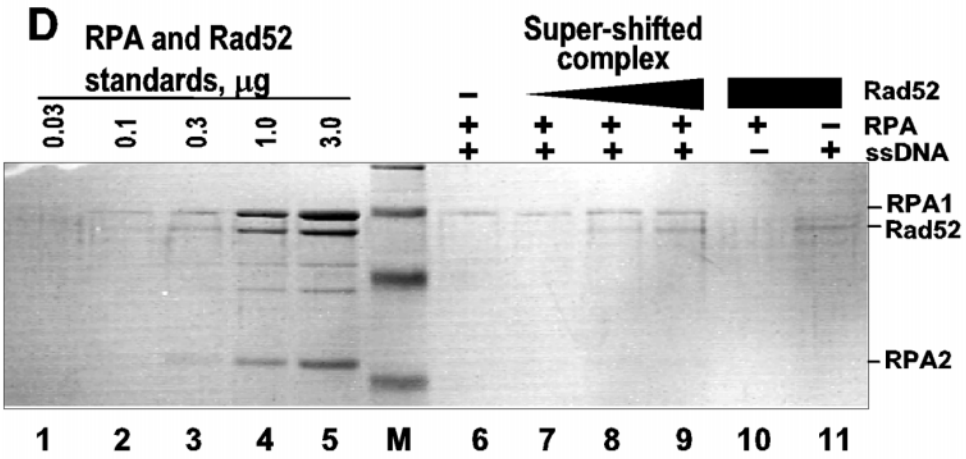
D
RPA and Rad52 standards, μg
0.03
0.1
0.3
1.0
3.0
Super-shifted complex
Rad52
RPA
ssDNA
RPA1
Rad52
RPA2
1 2 3 4 5 M 6 7 8 9 10 11

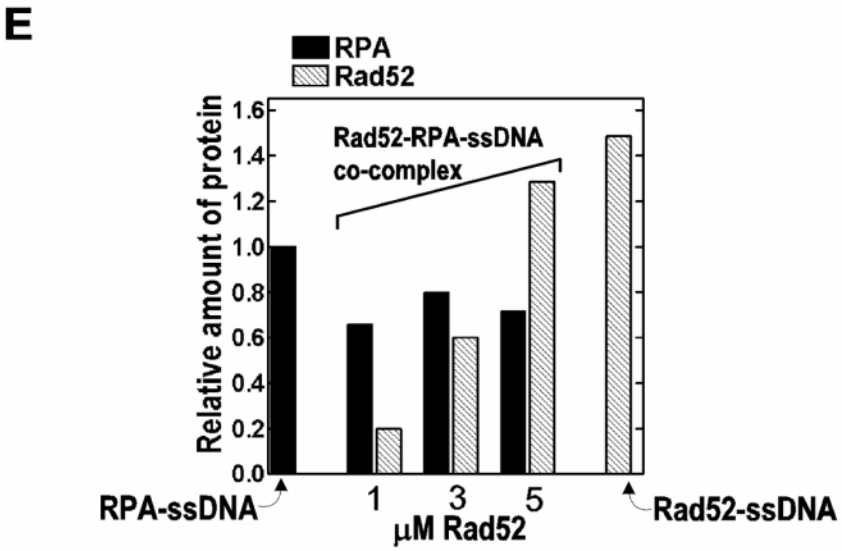
E
RPA
Rad52
Relative amount of protein
1.6
1.4
1.2
1.0
0.8
0.6
0.4
0.2
0.0
Rad52-RPA-ssDNA co-complex
RPA-ssDNA
1
3
5
μM Rad52
Rad52-ssDNA

Figure 8
Sugiyama & Kowalczykowski

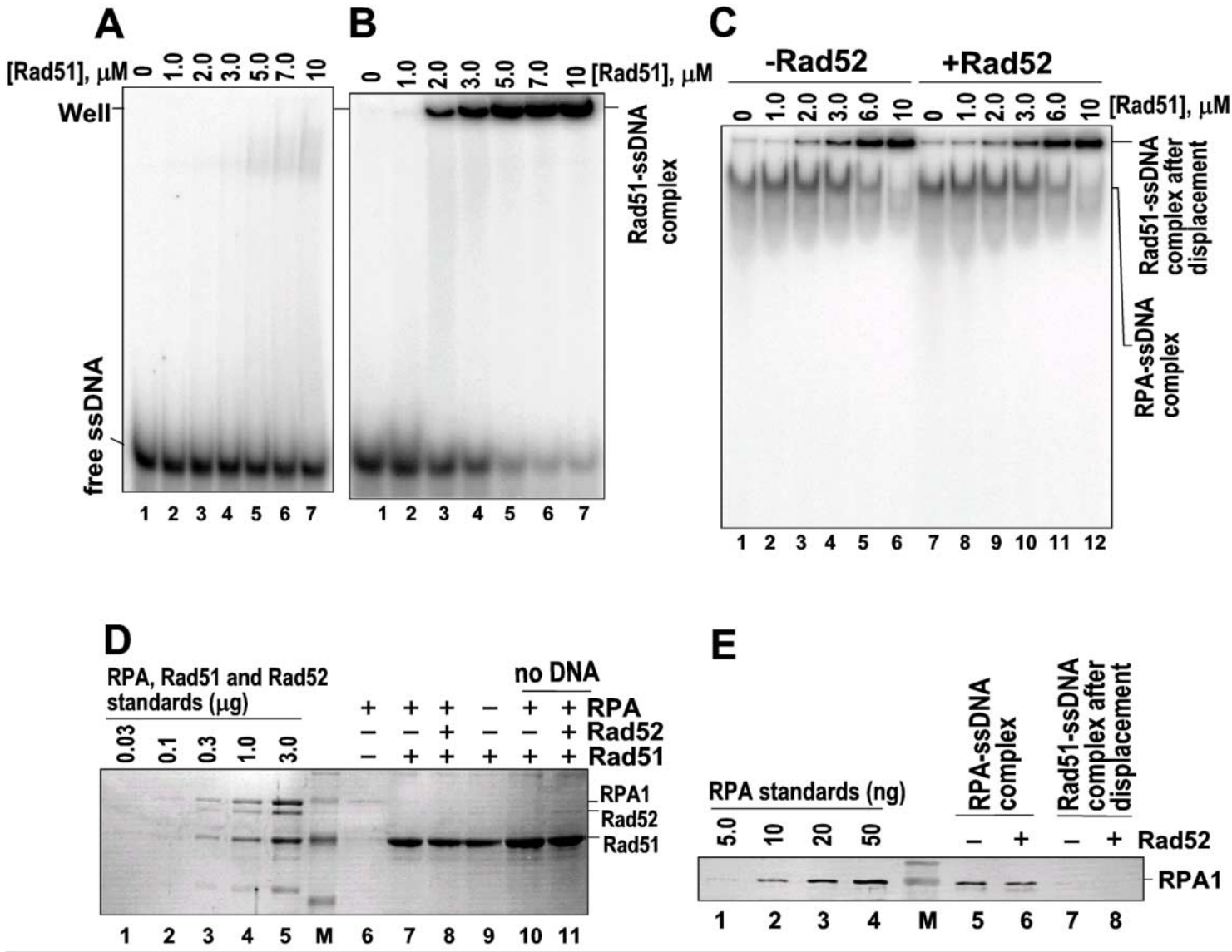

Fig. 9
Sugiyama & Kowalczykowski